Journal of Organometallic Chemistry 695 (2010) 2761–2767

Contents lists available at ScienceDirect

Journal of Organometallic Chemistry

journal homepage: www.elsevier.com/locate/jorganchem

Synthesis and reactivity of *trans*-*N*,*N*′-dimethyl-*meso*-octaalkylporphyrinogen Sm(II), Eu(II) and Yb(II) complexes: Metal-based influences on the reduction of *t*-butyl-1,4-diazabuta-1,3-diene☆

Andrew K.J. Dick [a], Alistair S.P. Frey [a], Michael G. Gardiner [a,*], Matthias Hilder [b], Adam N. James [a], Peter C. Junk [b], Suraphan Powanosorn [a], Brian W. Skelton [c], Jun Wang [a], Allan H. White [c]

[a] School of Chemistry, University of Tasmania, Private Bag 75, Hobart TAS 7001, Australia
[b] School of Chemistry, Monash University, VIC 3800, Australia
[c] School of Biomedical, Biomolecular and Chemical Sciences, Chemistry M313, The University of Western Australia, Crawley WA 6009, Australia

ARTICLE INFO

Article history:
Received 10 May 2010
Received in revised form
28 June 2010
Accepted 6 July 2010
Available online 14 July 2010

Keywords:
Lanthanide
Reduction chemistry
Macrocyclic ligands
1,4-Diazabuta-1,3-diene
Crystal structure
Steric effects

ABSTRACT

Sm(II), Eu(II) and Yb(II) complexes of doubly deprotonated *trans*-*N*,*N*′-dimethyl-*meso*-octaethylporphyrinogen were synthesised as tetrahydrofuran adducts (Sm and Eu, bis; Yb, mono) by metathetical exchange reactions of the dipotassium macrocyclic precursor complexes with the corresponding metal diiodides in tetrahydrofuran. The Sm and Eu complexes partially desolvate in non-coordinating solvents to give mono-tetrahydrofuran adducts. Subsequent reactions of the initial Eu(II) and Yb(II) complexes with 1,4-di-*t*-butyl-1,4-diazabuta-1,3-diene failed to yield complexes featuring the 1,4-diazabuta-1,3-diene binding to the lanthanide centres either as neutral Lewis base donors or reduced ligands, which contrasts with previous findings in the case of the analogous Sm(II) reaction. These outcomes are discussed in relation to the variety of Ln(III)–Ln(II) reduction potentials, coordination number and oxidation state dependent ionic radii of the metals and macrocycle–ancillary ligand steric interactions. The complexes were characterised by X-ray crystal structure determination, satisfactory microanalysis and NMR spectroscopy, where possible.

1. Introduction

The breadth of established reduction chemistry of organolanthanide complexes has been substantially widened in recent years. Major breakthroughs include access to the, so-called, non-traditional Ln(II) ions, and steric influences on both traditional Ln(II) metal-based reductions and ligand-based reductions of Ln(III) complexes [1]. In parallel, there has been renewed interest in the study of redox active ligands across a broad range of fundamental and applied inorganic chemistry [2]. The intersection of these contemporary research fields in the investigation of diimine complexes of the lanthanides has been of interest to a number of research groups and has led to the stabilisation of many unusual complexes and discovery of unusual reactivities [3].

The homoleptic 1,4-diazabuta-1,3-diene, R-DAB, complexes, [Ln(R-DAB)$_3$], have been the subject of on-going study with regard to formal oxidation state assignment [4]. The same ligand class has been examined in various studies of, mainly, heteroleptic lanthanocene complexes where variable neutral or reduced states of the R-DAB ligand have been reported. A non-lanthanocene example is the study of Sm and Yb complexes supported by the 1,4-bis(trimethylsilyl)cyclooctatetraenediyl dianion, affording the Sm(III) and Yb(II) complexes [{$C_8H_6(SiMe_3)_2$}Ln(R-DAB)(THF)] featuring radical anionic (for Sm(III)) and neutral (for Yb(II)) chelating R-DAB ligands (*t*-Bu-DAB and Ph-DAB, with 2,3-dimethyl substitution) [5]. Of relevance to this study, the differing reduced states of the R-DAB ligands were rationalised by the reducing strengths of the Ln(II) ions (strongest for Sm(II)). The inaccessibility of the Yb *t*-Bu-DAB complex was not discussed in this early report that lacked X-ray crystal structure determinations. More recent ytterbocene chemistry, discussed below, may indicate that steric issues play a role for the smaller Ln(II) ion in conjunction with the bulky cyclooctatetraenediyl ligand.

Interesting solvent-dependent redox activity was reported for decamethylytterbocene, with the Yb(III) complex [(C_5Me_5)$_2$Yb(*t*-Bu-DAB)] reverting to the Yb(II) complex [(C_5Me_5)$_2$Yb(THF)$_2$] and free *t*-Bu-DAB on addition of THF, Scheme 1 [6]. Central to the

☆ All authors dedicate this article to the memory of Prof. Dr. Herbert Schumann.

* Corresponding author. Tel.: +61 3 62262404; fax: +61 3 62262858.
E-mail address: michael.gardiner@utas.edu.au (M.G. Gardiner).

0022-328X/$ – see front matter
doi:10.1016/j.jorganchem.2010.07.004

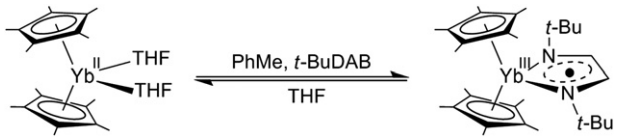

Scheme 1.

argument of steric interactions being influential on this reaction outcome is the observation that the analogous non-methylated system, $[(C_5H_5)_2Yb(t\text{-Bu-DAB})]$, is stable in the Yb(III) form in THF [7]. Significant lengthening of the Yb–N distance to the R-DAB ligand (2.390 vs 2.308 Å, average) is noted in the bulkier case, which further supports this premise. Temperature dependent solid state redox isomerism has more recently been reported for related complexes and multi-electron reductants have been developed that capitalise on these strain effects [3].

$[(C_5Me_5)_2Eu(THF)_2]$ was reported to react with *t*-Bu-DAB in toluene to give the Eu(II) complex $[(C_5Me_5)_2Eu(t\text{-Bu-DAB})]$ in which the *t*-Bu-DAB ligand bears no formal charge [8]. In contrast, the analogous reaction with C_6F_5-DAB (with 2,3-dimethyl substitution) in toluene gives the Eu(III) complex featuring the R-DAB ligand singly reduced. This complex reverts to the Eu(II) starting material upon addition of THF. The weak electron donating characteristics of the perfluorinated R-DAB ligand were implicated as a cause of the reversible redox chemistry.

We have previously reported the synthesis and reactivity of the bis(tetrahydrofuran) adduct of the Sm(II) complex [9] of the doubly deprotonated *trans-N,N′*-dimethyl-*meso*-octaethylporphyrinogen, $(Me_2N_4)^{2-}$, that we introduced into organometallic chemistry, $[(Me_2N_4)Sm(THF)_2]$, **1**. It forms an unusual 2:1 stoichiometric complex [10] on reaction with 1,4-di-*t*-butyl-1,4-diazabuta-1,3-diene, *t*-Bu-DAB, in toluene giving the dinuclear complex $[\{(Me_2N_4)Sm\}_2(t\text{-Bu-DAB})]$, **2**. Solution and solid state characterisation of **2** were consistent with the formulation of complex **2** as a Sm(III) species possessing an uncommon dianionic *t*-Bu-DAB ligand bridging the metal centres [11]. More unusual was the solvent triggered reversal to the Sm(II) starting material and free *t*-Bu-DAB upon the addition of tetrahydrofuran, Scheme 2. Such reversible Sm(III)/Sm(II) reactivity has very rarely been reported. More typical for Sm reactivity, as established through samarocenes [12], is the reduction of R-DAB ligands with $[(C_5Me_5)_2Sm(THF)_2]$ to afford mononuclear complexes featuring the chelating, singly reduced R-DAB ligand, $[(C_5Me_5)_2Sm(R\text{-DAB})]$.

The initial finding of the reversible Sm(III)/Sm(II) reactivity with $[(Me_2N_4)Sm(THF)_2]$ **1** left many unanswered issues in relation to the range of R-DAB complexes that can be accessed, in particular a more complete understanding of the reversible Sm(III)/Sm(II) behaviour of these complexes and whether such reactivity can be exploited in novel reduction chemistry applications. In this report we have investigated the formation of analogous Eu(II) and Yb(II) complexes and their reactivity with the same R-DAB ligand. These two systems were targeted due to the, i, similar metal ionic radii but lower reduction potential of the former relative to Sm(II), and, ii, smaller metal ionic radii of the latter.

2. Experimental section

2.1. General

Unless stated, all manipulations of complexes were carried out under an argon atmosphere by the use of standard Schlenk techniques or under nitrogen in a glove box (Innovative Technologies). $[\{(Me_2N_4)K_2(THF)_2\}_n]$, $[(Me_2N_4)Sm(THF)_2]$, **1**, *t*-Bu-DAB, $[(C_5Me_5)_2Sm]$, $EuI_2(THF)_2$ and $YbI_2(THF)_2$ were prepared according to literature procedures [10,13–16]. All other chemicals were obtained from Aldrich and used as received. ^1H and ^{13}C NMR spectra were recorded using a Varian Mercury Plus 300 spectrometer operating at 299.91 MHz (^1H) and 75.42 MHz (^{13}C). The ^1H NMR spectra were referenced to the residual ^1H resonances of chloroform-*d* (7.26), benzene-d_6 (7.15), toluene-d_8 (2.09) and THF-d_8 (1.73 or 3.75), and ^{13}C NMR spectra were referenced to the ^{13}C resonances of chloroform-*d* (77.2), benzene-d_6 (128.4), toluene-d_8 (20.4) and THF-d_8 (67.6 or 25.4). Full ^1H and ^{13}C NMR assignments of $[(Me_2N_4)Yb(THF)]$ **5** were made through gCOSY, gHMBC, gHMQC, NOESY and DEPT spectra. GC–MS spectra were performed using an HP5890 gas chromatograph equipped with an HP5790 Mass Selective Detector and a 25 m × 0.32 mm HPI column. Elemental analyses were performed by the Central Science Laboratory at the University of Tasmania (Carlo Erba EA1108 Elemental Analyser) or the Chemical and Analytical Services Pty. Ltd., Melbourne. I.R. spectra were recorded as Nujol mulls on NaCl plates using a Perkin–Elmer 1725X Fourier-transform infra-red spectrometer.

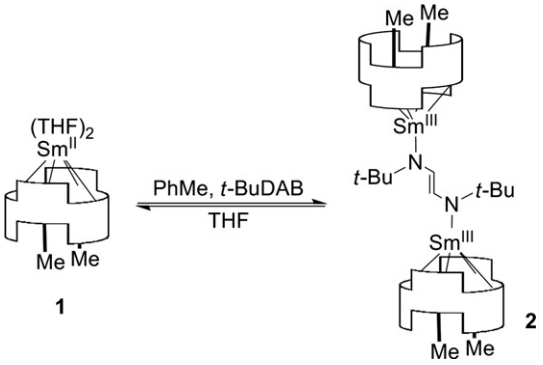

Scheme 2.

2.2. Synthesis of $[(Me_2N_4)Sm(THF)]$ *3*

Toluene (30 mL) was added to a mixture of $[(C_5Me_5)_2Sm]$ (0.17 mmol, 0.070 g) and $Li_2(Me_2N_4)$ (0.17 mmol, 0.096 g) and the mixture stirred for 5 h at 50 °C. The solution was concentrated in vacuo to 20 mL after this time and left to stand at room temperature overnight. This gave the title complex as a dark purple crystalline solid in low yield (ca. 5 mg). The ^1H NMR spectrum of the complete reaction mixture was characterised by very broad resonances spanning ca. −35 to 55 ppm ($\omega_{1/2}$ up to 400 Hz) and relatively weak resonances arising from diamagnetic impurities, including protonated macrocycle. ^1H NMR spectrum of the isolated solid of $[(Me_2N_4)Sm(THF)]$ **3** is different to this, being characterised by resonances of width and chemical shifts being intermediate between the crude reaction mixture and $[(Me_2N_4)Sm(THF)_2]$ **1**. Presumably the low yield of the mono(THF) solvate $[(Me_2N_4)Sm(THF)]$ **3** arises from incomplete desolvation of the samarocene reagent. A partial assignment is given (further assignment in the 0–10 ppm region could not be made owing to the purity of the sample obtained); ^1H NMR (298 K, C_6D_6): δ −25.6 (bs, 4H, CH_2), −9.85 (bs, 12H, CH_3), −7.83 (bs, 4H, CH_2), 12.60 (bs, 4H,=CH, pyrMe), 48.20 (bs, 6H, NCH_3).

2.3. Synthesis of $[(Me_2N_4)Eu(THF)_2]$ *4*

A solution of $EuI_2(THF)_2$ (0.63 mmol, 0.35 g) in THF (15 mL) was added via cannula to a suspension of $[\{(Me_2N_4)K_2(THF)_2\}_n]$ (0.63 mmol, 0.50 g) in THF (15 mL) with stirring. The colour changed from beige to yellow with the formation of pale solids. Stirring was

continued overnight, solvent was removed in vacuo and the solids extracted twice via filter cannula with toluene (20 and 10 mL). The solvent was removed in vacuo, THF (15 mL) added and the mixture warmed to effect dissolution. The warm solution was cooled to ambient temperature overnight, then stood overnight at −20 °C to complete crystallisation. Removal of the supernatant and drying in vacuo afforded the product as bright yellow prisms which were suitable for X-ray crystal structure determination (0.41 g, 75%). The paramagnetic behaviour of the complex prevented meaningful assignment of NMR spectra. Anal. Calc. for $C_{46}H_{70}N_4O_2Eu$: C, 64.02; H, 8.18; N, 6.49. Found: C, 63.85; H, 8.25; N, 6.51%.

2.4. Synthesis of [(Me$_2$N$_4$)Eu(THF)] **5**

[(Me$_2$N$_4$)Eu(THF)$_2$] **4** (2.4×10^{-4} mol, 0.21 g) was dissolved in toluene (3 mL) and allowed to stand at ambient temperature for 6 days, during which time large yellow prisms of the title compound formed. The supernatant was removed via cannula and the product dried in vacuo (0.17 g, 90%). The paramagnetic behaviour of the complex prevented meaningful assignment of NMR spectra. Suitable crystals for X-ray crystal structure determination were subsequently grown from benzene. Anal. Calc. for $C_{42}H_{62}N_4OEu$: C, 63.78; H, 7.90; N, 7.08. Found: C, 63.57, H, 7.46; N, 7.24%.

2.5. Synthesis of [(Me$_2$N$_4$)Yb(THF)] **6**

A solution of $YbI_2(THF)_2$ (4.6 mmol, 2.63 g) in THF (40 mL) was added via cannula to a suspension of [{(Me$_2$N$_4$)K$_2$(THF)$_2$}$_n$] (4.6 mmol, 2.94 g) in THF (40 mL) with stirring at room temperature. The reaction was stirred continuously overnight resulting in a yellow slurry and the mixture evaporated to dryness. Toluene (50 mL) was added, the solution filtered and the product crystallised by concentration as yellow prisms which were suitable for X-ray crystal structure determination (2.50 g, 70%). Subsequently, repeat syntheses have involved a final recrystallisation from THF as this led to improved removal of the potassium iodide by-product analogously to the Eu synthesis above. ^{1}H NMR (298 K, C_6D_6): δ 0.75 (t, 12H, CH_3), 0.90 (t, 12H, CH_3), 1.14 (s, 4H, THF), 1.75 (m, 4H, CH_2), 1.90 (m, 4H, CH_2), 2.18 (m, 8H, CH_2), 3.20 (s, 10H, NCH_3 and THF), 5.94 (s, 4H,=C*H*, pyrMe), 6.36 (s, 4H,=C*H*, pyr). ^{13}C NMR (298 K, C_6D_6): δ 8.6 (*C*H$_3$), 8.8 (*C*H$_3$), 24.4 (*C*H$_2$), 24.7 (THF), 32.2 (*C*H$_2$), 33.0 (NCH$_3$), 45.2 (*meso-C*), 68.3 (THF), 103.7 (β-*C*H, pyr), 105.6 (β-*C*H, pyrMe), 144.8 (α-*C*, pyr), 145.5 (α-*C*, pyr). Anal. Calc. for $C_{42}H_{62}N_4OYb\cdot C_7H_8$: C, 65.09; H, 7.80; N, 6.20. Found: C, 64.95; H, 7.77; N, 6.29%.

2.6. X-ray structure determinations for compounds **3**, **4**, **5** and **6**

Diffractometer data were measured with Bruker SMART, **3** (*T* ca. 152(2) K), Nonius Kappa, **6** (*T* ca. 173(2) K), or Enraf-Nonius CAD4, **4** and **5** (*T* ca. 193(2) K), instruments; monochromatic Mo Kα radiation; $\lambda = 0.71073$ Å. Neutral atom complex scattering factors were employed within the SHELX97 program systems [17]. The structures were solved by direct methods with SHELXS-97, refined using full-matrix least squares routines against F^2 with SHELXL-97 [18] and visualised using X-SEED [19]. All non-hydrogen atoms were refined anisotropically with the exception of a disordered toluene solvent molecule for **6**, see below. All hydrogen atoms were placed in calculated positions and refined using a riding model with fixed C–H distances of 0.95 Å (sp^2C–H) and 0.98 Å (CH$_3$), and U_{iso}(H) = 1.2U_{eq}(C) (sp^2) and 1.5U_{eq}(C) (sp^3). Pertinent data and results are given below and in Table 1 and Figs. 1 and 2. Disorder of the toluene solvent molecules in the structures of **3** and **6** were apparent in difference maps, which were modelled as two sets of sites with occupancies set at 0.5 after trial refinement and with geometries restrained to ideal values, for **3**, or refined with complementary occupancies for the two components. One *meso*-ethyl group in **3** was also modelled as being disordered over two sets of sites with the refined complementary occupancies for the two components.

Crystal data for **3**: $C_{49}H_{70}N_4OSm$, $M = 881.44$, triclinic, space group $P\bar{1}$, $a = 12.4750(10)$, $b = 14.015(2)$, $c = 14.588(2)$ Å, $\alpha = 70.959(3)$, $\beta = 66.897(2)$, $\gamma = 81.641(3)^\circ$, $V = 2217.2(5)$ Å^3, $Z = 2$, $D_c = 1.320$ g cm^{-3}, specimen: purple bar, 0.42 × 0.17 × 0.16 mm, 46933 measured reflections, $R_{int} = 0.040$, $R_1 = 0.0498$ for 16951 observed data ($(I) > 2\sigma(I)$), $wR_2 = 0.1389$, and GOOF = 1.062 for all data (22730).

Crystal data for **4**: $C_{46}H_{70}N_4O_2Eu$, $M = 863.02$, orthorhombic, space group *Pbcn*, $a = 21.422(4)$, $b = 10.646(2)$, $c = 18.569(4)$ Å, $V = 4234.7(15)$ Å^3, $Z = 4$, $D_c = 1.354$ g cm^{-3}, specimen: yellow prism, 0.30 × 0.30 × 0.30 mm, 3710 measured reflections, $R_{int} = 0.020$, $R_1 = 0.0295$ for 2851 observed data ($(I) > 2\sigma(I)$), $wR_2 = 0.826$, and GOOF = 1.068 for all data (3706).

Crystal data for **5**: $C_{45}H_{65}N_4OEu$, $M = 829.97$, monoclinic, space group *C*2/*c*, $a = 39.698(8)$, $b = 11.060(2)$, $c = 21.190(4)$ Å, $\beta = 118.21(3)^\circ$, $V = 8199(3)$ Å^3, $Z = 8$, $D_c = 1.345$ g cm^{-3}, specimen: yellow prism, 0.40 × 0.30 × 0.30 mm, 7380 measured reflections, $R_{int} = 0.032$, $R_1 = 0.0260$ for 6500 observed data ($(I) > 2\sigma(I)$), $wR_2 = 0.0706$, and GOOF = 1.101 for all data (7161).

Crystal data for **6**: $C_{49}H_{70}N_4OYb$, $M = 904.13$, triclinic, space group $P\bar{1}$, $a = 12.3535(2)$, $b = 14.0940(2)$, $c = 14.5381(2)$ Å, $\alpha = 70.4430(10)$, $\beta = 67.4790(10)$, $\gamma = 81.7390(10)^\circ$, $V = 2202.96(6)$ Å^3, $Z = 2$, $D_c = 1.363$ g cm^{-3}, specimen: pale yellow rod, 0.10 × 0.05 × 0.04 mm, 24269 measured reflections, $R_{int} = 0.040$, $R_1 = 0.0311$ for 9511 observed data ($(I) > 2\sigma(I)$), $wR_2 = 0.0811$, and GOOF = 1.041 for all data (10270).

3. Results and discussion

3.1. Complex synthesis

Metathetical exchange of [{(Me$_2$N$_4$)K$_2$(THF)$_2$}$_n$] with europium(II) and ytterbium(II) diiodide in THF at room temperature gave the corresponding new lanthanide(II) complexes and two equivalents of potassium iodide, Scheme 3. The removal of potassium iodide was effected by reducing the reaction mixtures to dryness in vacuo followed by extraction into toluene, again followed by reducing the solution to dryness. Subsequent recrystallisation from hot THF gave the complexes as yellow crystalline solids in high yield as a bis(THF) adduct for Eu, [(Me$_2$N$_4$)Eu(THF)$_2$], **4**, and mono(THF) adduct in the case of Yb, [(Me$_2$N$_4$)Yb(THF)], **6**. Attempts to filter from the metathesis reaction mixture as a solution in THF, concentration and subsequent crystallisation results in the precipitation of potassium iodide along with the desired complexes.

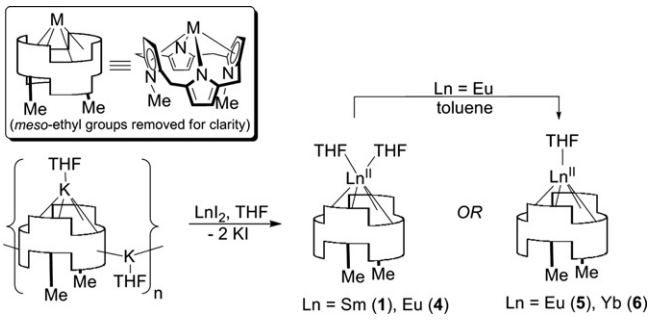

Scheme 3.

Table 1
Selected bond lengths (Å) and angles (°) for [(Me_2N_4)ML], **1**–**6**, along with [(Me_2N_4)SmMe].

	1 M = Sm(II), L = $(THF)_2$	**3** M = Sm(II), L = THF	M = Sm(III), L = Me	**2** M = Sm(III), L = μ-(*t*-Bu-DAB)	**4** M = Eu(II), L = $(THF)_2$	**5** M = Eu(II), L = THF	**6** M = Yb(II), L = THF
M-N(pyr)	2.6671(16)	2.566(2), 2.557(2)	2.478(3)	2.504(3)–2.545(3)	2.665(3)	2.561(2), 2.584(2)	2.485(2), 2.471(2)
M-centroid (pyrMe)	2.75_6	2.66_8, 2.68_7	2.59_3, 2.60_9	2.65_4–2.69_6	2.75_7	2.69_8, 2.70_3	2.61_6, 2.64_4
M-O/C/N (donor atom of ancillary ligand)	2.6552(14)	2.544(2)	2.424(5)	2.241(3), 2.251(3)	2.659(2)	2.528(2)	2.441(2)
N(pyr)-M-N(pyr)	120.03(7)	125.56(7)	127.82(9)	121.7(1), 123.1(1)	119.20(11)	124.80(7)	128.82(8)
Metallocene bend angle	154.4_4	163.6_4	168.8_6	161.5_3–161.5_4	154.1_8	162.7_0	169.4_5
pyr ring tilt angle	50.3_7	49.4_4, 55.6_0	50.1_5	45.1_0–53.8_2	50.4_4	52.9_4, 55.5_5	46.7_6, 52.6_2
pyrMe ring tilt angle	70.0_3	77.8_1, 78.3_0	78.8_1, 80.5_7	77.0_5–78.9_5	73.2_6	75.7_0, 77.2_1	80.1_2, 80.1_3
distance of M above *meso*-C plane	1.48_1	1.26_1	1.14_9	1.34_4	1.48_7	1.30_0	1.12_7

The new complexes [(Me_2N_4)Eu$(THF)_2$] **4** and [(Me_2N_4)Yb(THF)] **6** have been characterised by X-ray crystal structure determination, satisfactory microanalysis and, in the case of **6**, by ^{1}H and ^{13}C NMR spectroscopy. NMR spectroscopy was not informative for **4** due to the extreme line-broadening effect of the highly paramagnetic Eu(II) centre. Complexes **4** and **6** are soluble in THF, toluene and benzene.

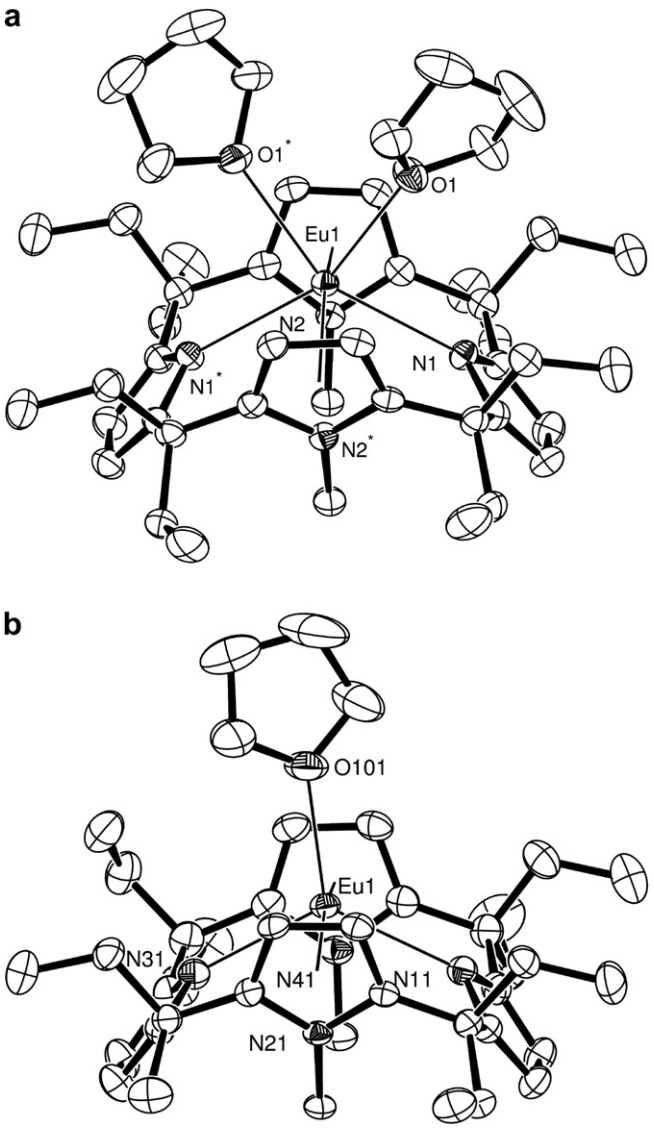

Fig. 1. Molecular structures of [(Me_2N_4)Eu$(THF)_2$] **4** and [(Me_2N_4)Eu(THF)] **5**. 50% probability amplitude displacement ellipsoids are shown for the non-hydrogen atoms. H atoms omitted for clarity.

In the case of the larger Eu(II) ion in complex **4**, partial desolvation to the mono(THF) adduct, [(Me_2N_4)Eu(THF)] **5**, is observed in toluene and benzene. Thus, solutions of **4** in benzene or toluene deposited yellow crystals of the mono(THF) adduct **5** upon standing at room temperature for 6 days, Scheme 3. The new complex was again characterised by X-ray crystal structure determination and satisfactory microanalysis. In the case of the similarly sized Sm(II) analogue, related conversion to the mono(THF) adduct [(Me_2N_4)Sm(THF)], **3**, is noted when [(Me_2N_4)Sm$(THF)_2$] **1** is crystallised from toluene. However, this is not a clean reaction and has proven to be poorly reproducible, preventing full characterisation of the mono(THF) adduct at this stage.

Characterisation of [(Me_2N_4)Sm(THF)] **3** rests on an X-ray crystal structure determination and partial ^{1}H and ^{13}C NMR spectroscopic analysis of samples obtained from a low yielding isolation from the reaction of [$(C_5Me_5)_2$Sm] with $(Me_2N_4)Li_2$ in toluene. The analogous reaction performed in THF using the THF adduct [$(C_5Me_5)_2$Sm$(THF)_2$] has been reported by us [9] as an unusual pentamethylcyclopentadienyl elimination reaction route to [(Me_2N_4)Sm$(THF)_2$] **1**. This reaction promised to offer an extended route into macrocyclic complexes of the $(Me_2N_4)^{2-}$ ligand across the whole series (where metathetical exchanges involving LnX_3 salts and direct macrocycle metallations have universally failed thus far). For the new unsolvated reaction reported here, presumably the sublimed sample of [$(C_5Me_5)_2$Sm] had not been exhaustively desolvated to remove all the coordinated THF, which accounts for the isolation of small amounts of [(Me_2N_4)Sm(THF)] **3**. The unsolvated reaction is thought to have provided access to the unsolvated macrocycle complex [(Me_2N_4)Sm] on the basis of the crude reaction product being spectroscopically identical to [(Me_2N_4)Sm$(THF)_2$] **1** upon addition of THF. However, the isolation of [(Me_2N_4)Sm] in pure form remains unachieved at this stage to verify this inference, even when this ligand exchange reaction was repeated with a rigorously desolvated [$(C_5Me_5)_2$Sm] sample. The ^{1}H NMR spectrum of the crude reaction mixture giving [(Me_2N_4)Sm(THF)] **3** by crystallisation from toluene is identical to the small amount of **3** isolated from the unsolvated ligand exchange route. Similar trends in the paramagnetic shift effects in [(Me_2N_4)Sm(THF)] **3** due to the Sm(II) centre are noted compared to those for [(Me_2N_4)Sm$(THF)_2$] **1**, with the exception that the magnitude of these shift effects are increased and greater line widths are seen. Both of these effects are consistent with the increased effects of the paramagnetic Sm(II) ion in the less solvated complex, where the bond distances to the macrocycle are shorter, see below.

3.2. Structural analysis

A number of features of the $(Me_2N_4)^{2-}$ ligand system are qualitatively shown by the three-dimensional representations of its

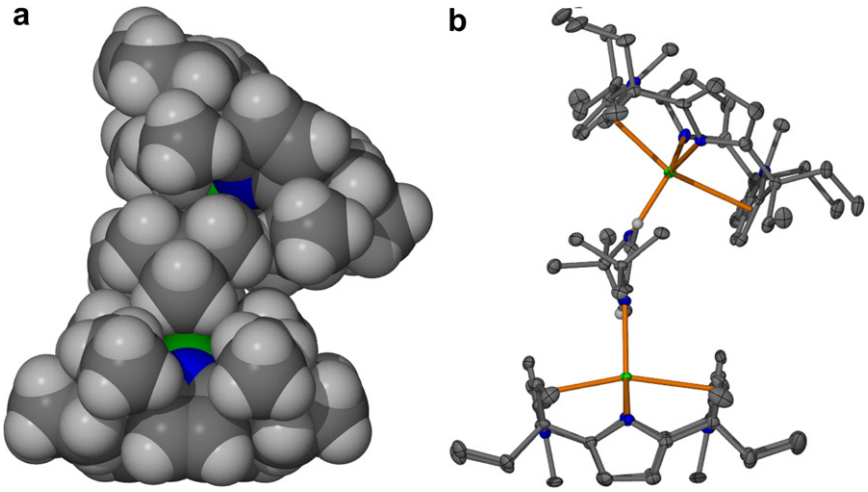

Fig. 2. Spacefilling (a) and thermal ellipsoid (b) representations of [{(Me_2N_4)Sm}$_2$(*t*-Bu-DAB)] **2** (viewed along the binding groove of the macrocycle at the bottom).

complexes **3**–**6** shown in Scheme 3. The macrocycle adopts the same 1,3-alternate conformation as the neutral ligand [20]. The metal is bound within the cavity by the two anionic pyrrolide ("pyr") nitrogen centres that act as a σ donors and displays η^5-interactions with the two *N*-methylpyrrolyl rings ("pyrMe"), as previously reported by us in a number of instances [21]. Whilst the situation is not always so simple, this arrangement is also found for the majority of complexes of the parent tetraanionic deprotonated *meso*-octaalkylporphyrinogen ligand class with large metals [22]. In this case, the *N*-methyl groups of the modified macrocyclic ligand extend towards one face of the macrocyclic plane, blocking access to the metal centre from the underside of the complex which prohibits the opportunity to form binuclear complexes.

THF solvent molecules are coordinated to the metal centres at the binding groove of complexes **3**–**6**. The Sm(II) and Eu(II) complexes **1** and **4** obtained from THF solutions bear two THF molecules, whilst the Yb(II) complex **6** accommodates only one THF molecule. The differing numbers of coordinated THF molecules in this series crystallised from THF are due to the interplay of macrocycle bulk and the difference in ionic radius of the metal centres, which is explained in detail below owing to the relevance of this argument to the outcome of their reactions with *t*-Bu-DAB.

Not so apparent from the representations in Scheme 3 is the depth in which the metal centres reside in the macrocyclic cavity. Fig. 1 shows the molecular structures of the bis- and mono(THF) adducts of the Eu(II) complexes **4** and **5**, which highlight this important feature. [(Me_2N_4)Eu(THF)$_2$] **4** is isomorphous to the previously reported [(Me_2N_4)Sm(THF)$_2$] **1** [9]. The mono(THF) adducts are all similar in structure, with the toluene solvates of [(Me_2N_4)Sm(THF)] **3** and [(Me_2N_4)Yb(THF)] **6** being isomorphous. The Eu(II) analogue **5** has lattice benzene and exhibits different packing. Table 1 gives a summary of important geometric parameters for the series of complexes.

The depth of the metal in the macrocyclic cavity significantly limits the binding of ancillary ligands, particularly for smaller metals. Clearly, this has an effect on the formation of only the mono (THF) adduct in the case of Yb(II) in comparison to the larger Sm(II) and Eu(II) ions forming bis(THF) adducts. Three useful geometric parameters describing the steric limitations on ancillary ligand binding in this series of complexes are, i, the distance that the metal sits above the mean square plane defined by the four *meso*-carbon centres of the macrocycle, ii, the "tilt angles" of the pyrrolide (pyr) and *N*-methylpyrrolyl (pyrMe) rings with respect to this macrocyclic plane, and, iii, the "metallocene bend angle" defined here as the centroid-M-centroid angle to the η^5-bound *N*-methylpyrrolyl rings of the macrocycle. Of note, these bend angles reveal only slight bending relative to lanthanocenes. Analysis of Table 1 reveals the clear trends in metal ion size across the series of Ln(II) complexes **1**, **3**–**6**, including oxidation state and coordination number effects that correlate well with the metal ion radii. For example, the decrease in ionic radius for a coordination number reduction of one has been determined in a crystallographic survey of Eu(II) compounds [23] to be ca. 3.7% (1.35–1.30 Å from coordination number 10 to 9). The Eu–N(pyr) and Eu–O bond lengths in the bis(THF) adduct **4** are longer than those observed in mono(THF) adduct **5** by 3.1–5.2%, consistent with this reduction in coordination number. Similar trends are observed in the isostructural Sm(II) complexes [(Me_2N_4)Sm(THF)$_2$] **1** and [(Me_2N_4)Sm(THF)] **3** [9]. The distance of the metal centre from the plane of the macrocycle appears to be very sensitive to both the ionic radius of the metal and steric strain between the macrocycle and ancillary ligands, see below.

3.3. *t*-Bu-DAB ligand exchange reactivity of complexes *4* and *6*

The increased steric influences of the $(Me_2N_4)^{2-}$ macrocyclic ligand on ancillary ligands relative to the bis(pentamethylcyclopentadienyl) ligand set has previously been established through a number of comparative structural studies [9,21]. In particular, the macrocycle exhibits a relatively short binding groove for accommodating ancillary ligands that is limited by the *meso*-ethyl substituents that have no spatial counterparts in metallocene chemistry.

The reversible, solvent-mediated Sm(III)/Sm(II) system discovered for the [{(Me_2N_4)Sm}$_2$(*t*-Bu-DAB)] **2**/[(Me_2N_4)Sm(THF)$_2$] **1** couple is extremely unusual, Scheme 2 [10]. The presence of the bridging μ-(*t*-Bu-DAB)$^{2-}$ ligand in **2** indicates signs of steric strain relief having driven the reaction outcome (in adopting a non-chelated structure). The ability of *t*-Bu-DAB to adopt a chelated radical anion would not be feasible owing to the interactions between the macrocycle and the *t*-Bu substituents of the R-DAB ligand (as the width of the ancillary ligand in this bidentate form would exceed the length of the binding groove for ancillary ligands). Still, the complex displays quite a highly congested nature in this compromised *t*-Bu-DAB binding mode.

The oxidation of Sm(II) to Sm(III) upon reduction of *t*-Bu-DAB introduces a structural subtlety that may be responsible for the reversible redox chemistry. The ionic radius of the samarium centre decreases with the removal of an electron from Sm(II) to Sm(III). The smaller Sm(III) centre then resides substantially further within

the macrocyclic cavity, making less coordination sphere available for binding at the top of the macrocycle and resulting in increased steric strain between the reduced 1,4-diazabuta-1,3-diene and the macrocycle. This implies a balance whereby the forward reaction (oxidation of Sm(II) to Sm(III)) is favoured on electronic grounds, whilst the reverse reaction is favoured on steric grounds. The reverse reaction allows the relief of strain between the deeply bound Sm(III) centre and the reduced 1,4-diazabuta-1,3-diene along with the added coordination of two THF molecules to the less deeply bound Sm(II) centre.

Included in Table 1 are two comparative Sm(III) complexes [10,21,24] with minimal, [(Me_2N_4)Sm(Me)], and significant strain, [{(Me_2N_4)Sm}$_2$(*t*-Bu-DAB)], **2**, between the macrocycle and the ancillary ligand. Specifically, in the latter case, between the *N*-*t*-Bu and *meso*-ethyl substituent region, see Fig. 2(a). Apparent is the contraction in metal radius upon oxidation of Sm(II) to Sm(III) discussed above and the variation in Sm to macrocycle contacts between the Sm(III) complexes associated with the steric strain of complex **2**. The deeper position of the Sm(III) centre in **2** relative to Sm(II) complex **3** with the same coordination number is reflected in most of the relevant comparators given in Table 1. The distance of the Sm(III) centre above the plane of the macrocycle in [{(Me_2N_4)Sm}$_2$(*t*-Bu-DAB)] **2** relative to the unstrained complex [(Me_2N_4)Sm(Me)] is a good indicator of the strain existing in the former complex. Fig. 2 also illustrates how the steric interactions between each *t*-Bu group of the μ-(*t*-Bu-DAB) ligand and each macrocycle in the dinuclear complex dictates the overall shape of the complex; the "top" macrocycle is tilted to the side in order for two of the triangularly disposed methyl groups of the *t*-Bu-DAB ligand each to mesh into the narrow ends of the macrocyclic binding grooves. The consequence of this is a significantly non-planar arrangement of the μ-(*t*-Bu-DAB) ligand core that would otherwise not be expected to be favourable, Fig. 2(b). Similar lowered symmetry was noted [24] for the structurally related [{(Me_2N_4)Sm}$_2$(μ-*t*-Bu-C═PP═C-*t*-Bu)] prepared through reductive coupling of *tert*-butyl phosphaalkyne, *t*-BuC≡P, with [(Me_2N_4)Sm(THF)$_2$] **1**.

To the best of our knowledge, reports of reversible Sm(III)/Sm(II) chemistry are restricted to, i, dinitrogen, and aromatic and non-aromatic hydrocarbon complexes of decamethylsamarocene [25], and, ii, dinitrogen and ethylene complexes of tetrametallated porphyrinogens [26]. Reversible Sm(III)/Sm(II) reactivity has not been noted for [(C_5R_5)$_2$Sm(R-DAB)] [12]. As noted earlier, solvent-mediated reversible equilibria has been reported for Yb(III) bis(pentamethylcyclopentadienyl) [6], bis(indenyl) and *ansa*-indenyl R-DAB complexes [27], and a Eu(III) bis(pentamethylcyclopentadienyl) R-DAB complex [8]. The relative inaccessibility of the Sm chemistry is associated with both the larger size of the metal ion (minimising steric influences) and the more reducing nature of Sm(II) relative to Eu(II) and Yb(II).

If steric restrictions are responsible for the reversible redox behaviour of **1**/**2**, smaller 1,4-diazabuta-1,3-diene substituents should allow improved Sm to R-DAB interactions with the deeply bound Sm(III) centre. Thus, the complexes would be less liable to undergo the reverse reaction on steric grounds. Additionally, variations in the reduction potential of the Ln(II) ion and/or ionic radius should be influential. The outcomes and interpretations of our initial investigations of varying the metal properties along this principle are discussed below.

Eu(II) has an ionic radius very similar to that of Sm(II). Thus, [(Me_2N_4)Eu(THF)$_2$] **4** would be expected to present effectively the same portion of its coordination sphere to an incoming *t*-Bu-DAB molecule as the equivalent Sm(II) complex [(Me_2N_4)Sm(THF)$_2$] **1**. However, Eu(II) is a much weaker reducing agent than Sm(II) (reduction potentials −0.35 and −1.55 V vs NHE, respectively [28]). An attempted reaction between the Eu(II) precursor [(Me_2N_4)Eu(THF)$_2$] **4** and *t*-Bu-DAB was thus undertaken. A solution of **4** in benzene-d_6 was added to a solution of *t*-Bu-DAB in benzene-d_6 on an NMR scale producing no immediately visible sign of reaction. Partial removal of solvent in vacuo and standing at room temperature for 2 weeks produced yellow crystals of the mono-THF adduct [(Me_2N_4)Eu(THF)] **5** in high yield. Resonances in the ^{1}H NMR spectrum of the reaction mixture were extremely broadened due to the paramagnetic Eu(II) centre, making assignment impossible; only free *t*-Bu-DAB was clearly identifiable. Failure of *t*-Bu-DAB to react with the Eu(II) precursor contrasts with the analogous Sm(II) case [10]. We rationalise this according to the fact that the analogous dinuclear Eu(III) product [{(Me_2N_4)Eu}$_2${*t*-Bu-DAB}] would suffer from the same steric issues as the Sm(II) analogue without the strong forward reaction tendencies of the metal oxidation which drives the Sm(II) reaction. It was already established that [(Me_2N_4)Eu(THF)$_2$] **4** desolvates to [(Me_2N_4)Eu(THF)] **5** in benzene. Further, the observed lack of formation of a *t*-Bu-DAB adduct of Eu(II), [(Me_2N_4)Eu(*t*-Bu-DAB)] or perhaps a 2:1 stoichiometric product, is presumably a simple non-redox driven Lewis base competition between *t*-Bu-DAB and THF and/or is associated with a solubility-driven equilibrium.

Due to the increased effective nuclear charge, the ionic radius of Yb(II) is considerably smaller than Sm(II) and Eu(II). Therefore a Yb(II) centre is expected to reside deepest within the macrocyclic cavity. This results in less coordination sphere being available for subsequent reaction in the case of a Yb(II) complex (*viz.* [(Me_2N_4)Sm(THF)$_2$] **1** contains two THF molecules whilst [(Me_2N_4)Yb(THF)] **6** is observed with only one bound THF). Despite Yb(II) still being relatively strongly reducing (Yb(II) reduction potential −1.15 V vs NHE [28]), based on the outcome of the reaction of [(Me_2N_4)Eu(THF)$_2$] **4** with *t*-Bu-DAB described above, [(Me_2N_4)Yb(THF)] **6** would not be expected to be able to form either a Yb(II) or Yb(III) complex with *t*-Bu-DAB on steric grounds. Indeed, the attempted reaction between [(Me_2N_4)Yb(THF)] **6** and *t*-Bu-DAB in toluene was unsuccessful, with no colour change upon addition and only starting **6** being recovered upon removal of solvent.

Unique in our set of *t*-Bu-DAB reactions across Sm(II), Eu(II), and Yb(II) is that formation of the simple Lewis base adducts are not seen for both the relatively large Eu(II) and small Yb(II) cases, and reversible redox chemistry is observed for Sm(II). This behaviour contrasts with analogous lanthanocene reactions where *t*-Bu-DAB complex formation is always observed, solvent-mediated reversible redox behaviour is only observed for the smallest Ln(II) ion (Yb(II)) and the Eu(II) adduct is isolated. Both of these observations are consistent with the argument of steric limitations being influenced by changes to the ionic radii of the metal centres and the increased steric influence of the $(Me_2N_4)^{2-}$ ligand relative to the bis(pentamethylcyclopentadienyl) ligand set.

4. Conclusions

The preparation of the Eu(II) and Yb(II) complexes in this report has widened the range of lanthanide complexes for this modified doubly deprotonated *trans*-*N*,*N*′-dimethyl-*meso*-octaethylporphyrinogen ligand, which now includes the full breadth of traditional Ln(II) ions. While all attempts thus far to widen the chemistry to other lanthanides by metathetical exchange reactions with LnX_3 salts have been unsuccessful, extended application of a pentamethylcyclopentadienyl elimination reaction demonstrated for Sm(II) may overcome this limiting situation. The lack of reaction of [(Me_2N_4)Eu(THF)$_2$] and [(Me_2N_4)Yb(THF)] with *t*-Bu-DAB in toluene in comparison with our previously reported [(Me_2N_4)Sm(THF)$_2$] reactivity has highlighted the effects that metal size and reduction potential have on the outcomes of this reaction series. Without the

strongest Ln(II) to Ln(III) oxidation tendency in the case of Sm, THF outcompetes *t*-Bu-DAB as the ancillary ligand for Eu. Whereas for the relatively smaller Yb case, steric restrictions also had this effect, outweighing the normal strive for the formation of the Yb(III) ion by reduction of the *t*-Bu-DAB ligand. We are continuing to further investigate steric effects in these R-DAB reactions and are attempting to access further lanthanide complexes of this macrocyclic ligand through reactions of the newly accessible LnI_2 reagents. Exploring the anticipated higher reactivity of these complexes is likely to result in more highly strained reaction products and/or unusual reactivity patterns.

Acknowledgements

We thank the Australian Research Council for financial support of the early phase of this research (Large Grant) and the School of Chemistry (University of Tasmania) for support.

Appendix A. Supplementary material

CCDC 787166 and 787498-787500 contain the supplementary crystallographic data for **3**–**6**. These data can be obtained free of charge from The Cambridge Crystallographic Data Centre via www.ccdc.cam.ac.uk/data_request/cif. Supplementary data associated with this article can be found, in the online version, at doi:10.1016/j.jorganchem.2010.07.004.

References

[1] (a) W.J. Evans, J. Organomet. Chem. 647 (2002) 2;
(b) W.J. Evans, B.L. Davis, Chem. Rev. 102 (2002) 2119;
(c) M.N. Bochkarev, Coord. Chem. Rev. 248 (2004) 835;
(d) K. Izod, Angew. Chem. Int. Ed. 41 (2002) 743;
(e) G. Meyer, Angew. Chem. Int. Ed. 47 (2008) 4962;
(f) F. Nief, D. Turcitu, L. Ricard, Chem. Commun. (2002) 1646;
(g) W.J. Evans, K.J. Forrestal, J.W. Ziller, J. Am. Chem. Soc. 120 (1998) 9273;
(h) C. Ruspic, J.R. Moss, M. Schürmann, S. Harder, Angew. Chem. Int. Ed. 47 (2008) 2121;
(i) F. Jaroschik, A. Momin, F. Nief, X.F Le Goff, G.B. Deacon, P.C. Junk, Angew. Chem. Int. Ed. 48 (2009) 1117;
(j) F. Jaroschik, F. Nief, X.F. Le Goff, L. Ricard, Organometallics 26 (2007) 1123.
[2] For reviews and examples of recent articles, see: G. van Koten, K. Vrieze Adv. Organomet. Chem. 21 (1982) 151;
(a) K. Vrieze, J. Organomet. Chem. 300 (1986) 307;
(b) F.G.N. Cloke, Chem. Soc. Rev. 22 (1993) 17;
(c) N.J. Hill, I. Vargas-Baca, A.H. Cowley, Dalton Trans. (2009) 240;
(d) K. Ray, T. Petrenko, K. Wieghardt, F. Neese, Dalton Trans. (2007) 1552;
(e) M.M. Khusniyarov, T. Weyhermuller, E. Bill, K. Wieghardt, J. Am. Chem. Soc. 131 (2009) 1208.
[3] (a) K. Vasudevan, A.H. Cowley, Chem. Commun. (2007) 3464;
(b) A.A. Trifonov, I.A. Borovkov, E.A. Fedorova, G.K. Fukin, J. Larionova, N.O. Druzhkov, V.K. Cherkasov, Chem.—Eur. J. 13 (2007) 4981;
(c) I.L. Fedushkin, O.V. Maslova, E.V. Baranov, A.S. Shavyrin, Inorg. Chem. 48 (2009) 2355;
(d) A.A. Trifonov, Euro. J. Inorg. Chem. (2007) 3151.
[4] (a) F.G.N. Cloke, H.C. de Lemos, A.A. Sameh, J. Chem. Soc. Chem. Commun. (1986) 1344;
(b) M.N. Bochkarev, A.A. Trifonov, F.G.N. Cloke, C.I. Dalby, P.T. Matsunaga, R.A. Andersen, H. Schumann, J. Loebel, H. Hemling, J. Organomet. Chem. 486 (1995) 177.
[5] P. Poremba, F.T. Edelmann, J. Organomet. Chem. 549 (1997) 101.
[6] A.A. Trifonov, Y.A. Kurskii, M.N. Bochkarev, S. Muehle, S. Dechert, H. Schumann, Russ. Chem. Bull. Int. Ed. 52 (2003) 601.
[7] A.A. Trifonov, E.N. Kirillov, M.N. Bochkarev, H. Schumann, S. Muehle, Russ. Chem. Bull. Int. Ed. 48 (1999) 384.
[8] J.A. Moore, A.H. Cowley, J.C. Gordon, Organometallics 25 (2006) 5207.
[9] J. Wang, A.K.J. Dick, M.G. Gardiner, B.F. Yates, E.J. Peacock, B.W. Skelton, A.H. White, Eur. J. Inorg. Chem. (2004) 1992.
[10] J. Wang, R.I.J. Amos, A.S.P. Frey, M.G. Gardiner, M.L. Cole, P.C. Junk, Organometallics 24 (2005) 2259.
[11] A. Recknagel, M. Noltemeyer, F.T. Edelmann, J. Organomet. Chem. 410 (1991) 53.
[12] J. Scholz, M. Dlikan, D. Ströhl, A. Dietrich, H. Schumann, K.-H. Thiele, Chem. Ber. 123 (1990) 2279.
[13] J. Wang, M.G. Gardiner, E.J. Peacock, B.W. Skelton, A.H. White, Dalton Trans. (2003) 161.
[14] J.M. Kliegman, R.K. Barnes, Tetrahedron 26 (1970) 2555.
[15] W.J. Evans, L.A. Hughes, T.P. Hanusa, J. Am. Chem. Soc. 106 (1984) 4270.
[16] P.L. Watson, T.H. Tulip, I. Williams, Organometallics 9 (1990) 1999.
[17] T. Hahn (Ed.), International Tables for Crystallography, Kluwer Academic Publishers, Dordrecht, The Netherlands, 1995.
[18] G.M. Sheldrick, SHELX97, Programs for Crystal Structure Analysis. Universität Göttingen, Germany, 1998.
[19] L.J. Barbour, J. Supramol. Chem. 1 (2001) 189.
[20] Y.-S. Jang, H.-J. Kim, P.-H. Lee, C.-H. Lee, Tetrahedron Lett. 41 (2000) 2919.
[21] (a) J. Wang, M.G. Gardiner, B.W. Skelton, A.H. White, Organometallics 24 (2005) 815;
(b) N.W. Davies, A.S.P. Frey, M.G. Gardiner, J. Wang, Chem. Commun. (2006) 4853;
(c) A.S.P. Frey, M.G. Gardiner, D.N. Stringer, B.F. Yates, A.V. George, P. Jensen, P. Turner, Organometallics 26 (2007) 1299.
[22] (a) J. Jubb, S. Gambarotta, R. Duchateau, J.H. Teuben, J. Chem. Soc. Chem. Commun. (1994) 2641;
(b) E. Campazzi, E. Solari, C. Floriani, R. Scopelliti, Chem. Commun. (1998) 2603;
(c) J. Jubb, S. Gambarotta, J. Am. Chem. Soc. 116 (1994) 4477;
(d) E. Campazzi, E. Solari, R. Scopelliti, C. Floriani, Chem. Commun. (1999) 1617;
(e) T. Dubé, J. Guan, S. Gambarotta, G.P.A. Yap, Chem.—Eur. J. 7 (2001) 374;
(f) J.I. Song, S. Gambarotta, Angew. Chem. Int. Ed. Engl. 34 (1995) 2141;
(g) T. Dubé, S. Gambarotta, G. Yap, Organometallics 19 (2000) 121.
[23] R.D. Shannon, Acta Crystallogr. A32 (1976) 751.
[24] The nitrile adduct [(Me_2N_4)Sm(NC-*t*-Bu)] follows the same trend: M.G. Gardiner, A.N. James, C. Jones, C. Schulten, Dalton Trans. 39 (2010) 6864–6870.
[25] (a) W.J. Evans, T.A. Ulibarri, J.W. Ziller, J. Am. Chem. Soc. 110 (1988) 6877;
(b) W.J. Evans, T.A. Ulibarri, J.W. Ziller, J. Am. Chem. Soc. 112 (1990) 219;
(c) W.J. Evans, D.G. Giarikos, C.B. Robledo, V.S. Leong, J.W. Ziller, Organometallics 20 (2001) 5648;
(d) W.J. Evans, S.L. Gonzales, J.W. Ziller, J. Am. Chem. Soc. 116 (1994) 2600.
[26] (a) T. Dubé, S. Gambarotta, G.P.A. Yap, Angew. Chem. Int. Ed. 38 (1999) 1432;
(b) J. Guan, T. Dubé, S. Gambarotta, G.P.A. Yap, Organometallics 19 (2000) 4820.
[27] (a) A.A. Trifonov, E.A. Fedorova, G.K. Fukin, V.N. Ikorskii, Y.A. Kurskii, S. Dechert, H. Schumann, M.N. Bochkarev, Russ. Chem. Bull. Int. Ed. 53 (2004) 2736;
(b) A.A. Trifonov, E.A. Fedorova, V.N. Ikorskii, S. Dechert, H. Schumann, M.N. Bochkarev, Eur. J. Inorg. Chem. (2005) 2812.
[28] L.R. Morss, Chem. Rev. 76 (1976) 827.